

Supplementary Information

A Series of Mn(I) Photo-activated Carbon Monoxide-Releasing Molecules with Benzimidazole Coligands: Synthesis, Structural Characterization, CO Releasing Properties and Biological Activities

Mixia Hu,^{1,2,3} YaLi Yan,⁴ Baohua Zhu,^{1,2*} Fei Chang,¹ Shiyong Yu¹ and Gaole Alatan⁴

¹Chemistry and Chemical Engineering College, Inner Mongolia University, Hohhot 010021, China. ²Key Lab of Fine Organic Synthesis Inner Mongolia Autonomous Region, Hohhot 010021, China. ³College of Pharmacy, Inner Mongolia Medical University, Hohhot 010110, China. ⁴School of Life Sciences, Inner Mongolia University, Hohhot 010021, China

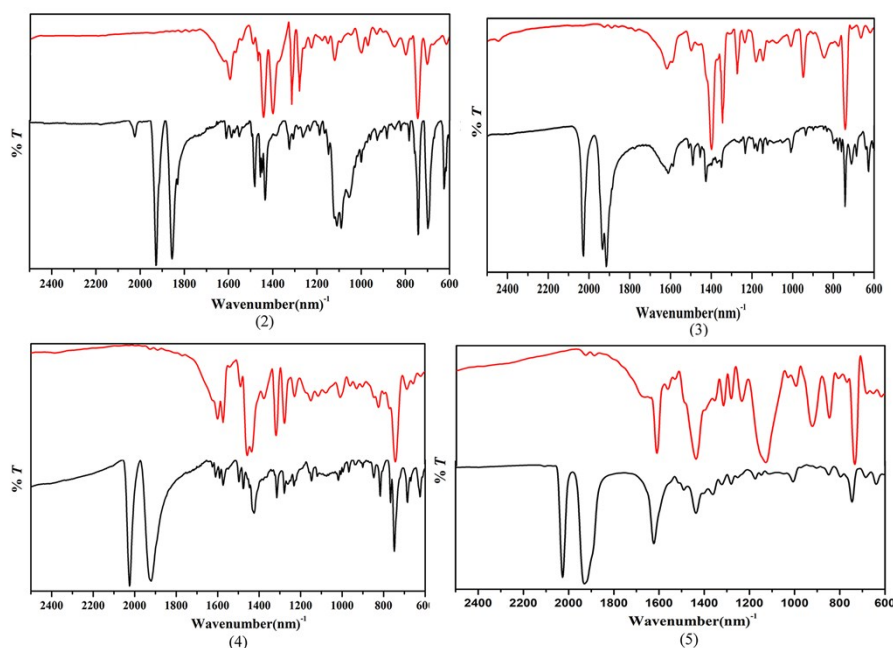


Fig. S1 IR spectrum of 1-5 (KBr disk) (black) and its photoproduct (red).

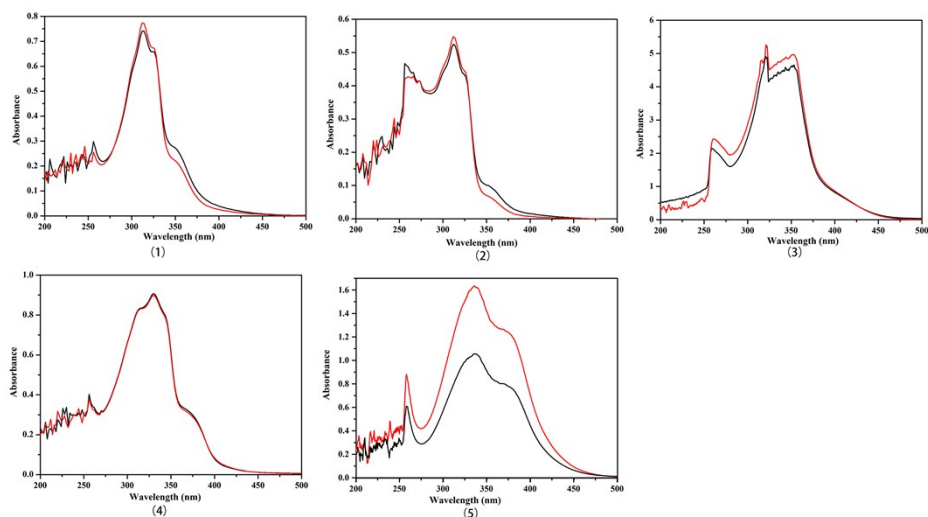
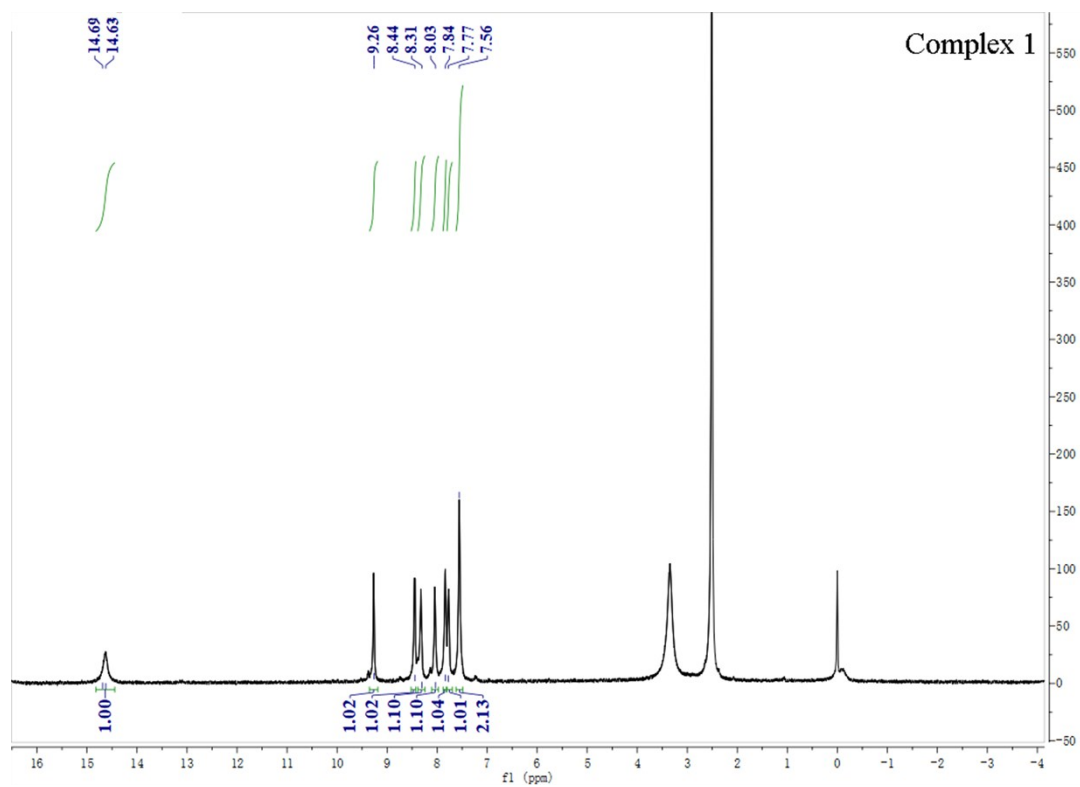
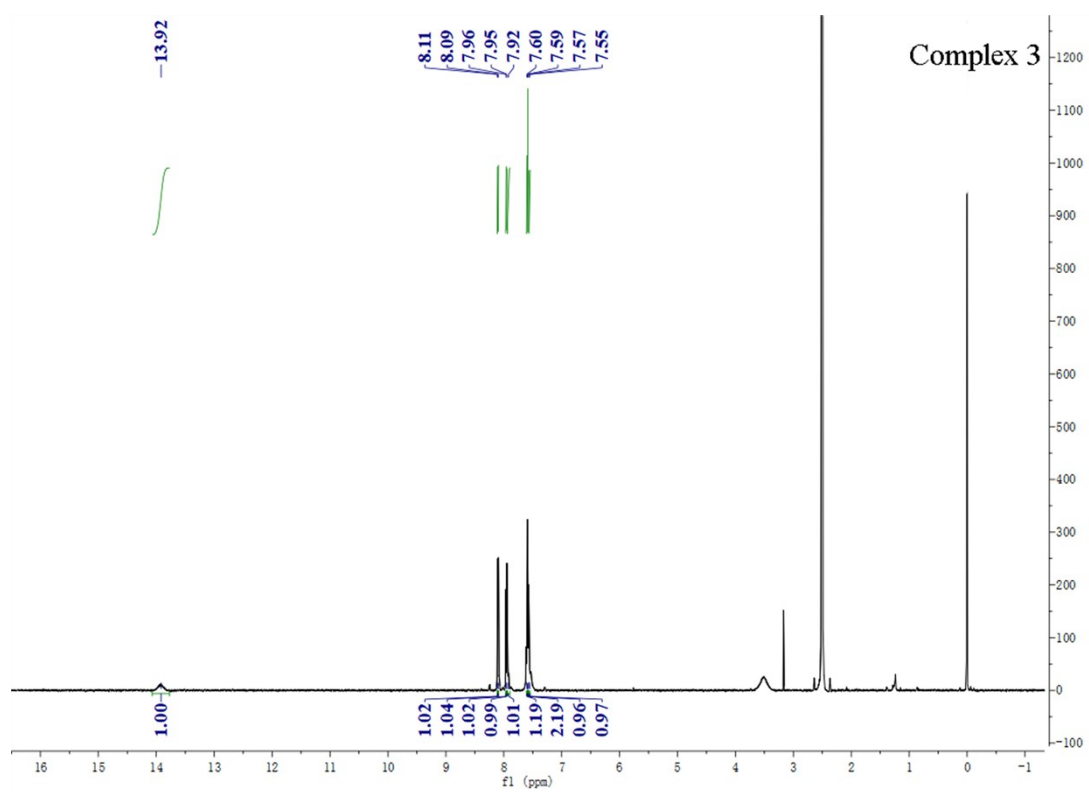
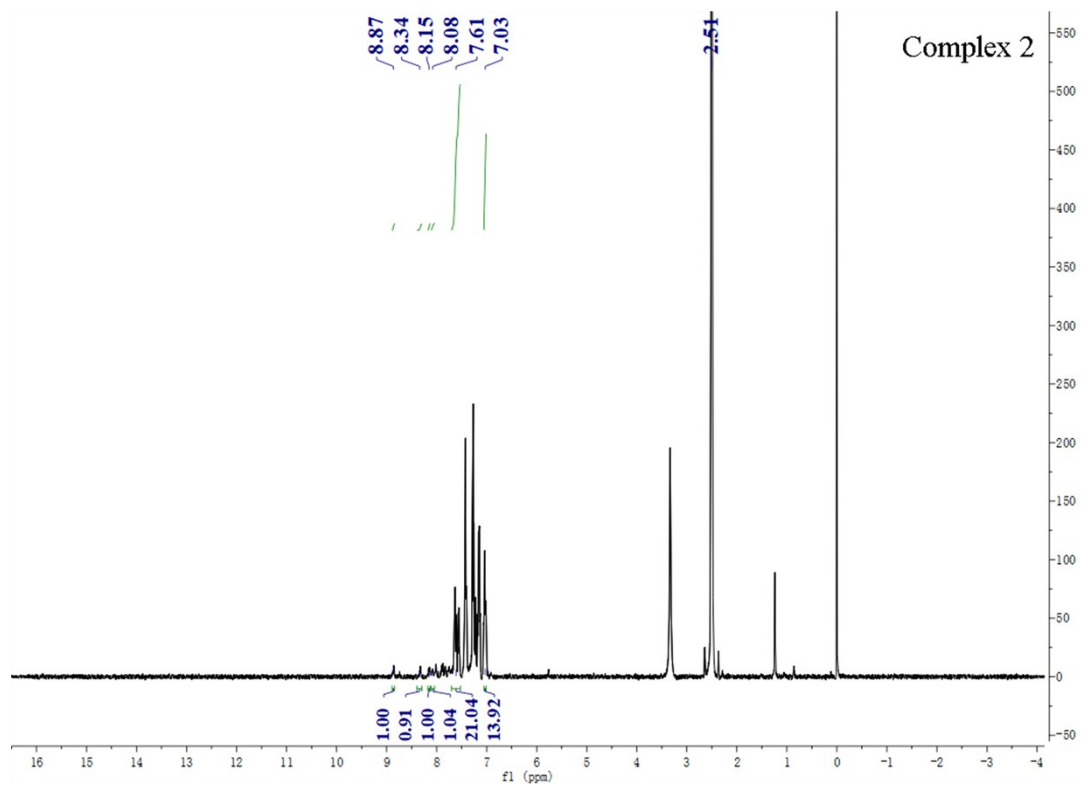


Fig. S2 The UV-vis absorption spectra of **1-5** in DMSO solution at room temperature (black) and The UV-vis absorption spectra of **1-5** in DMSO solution away from light for 24h (Red).





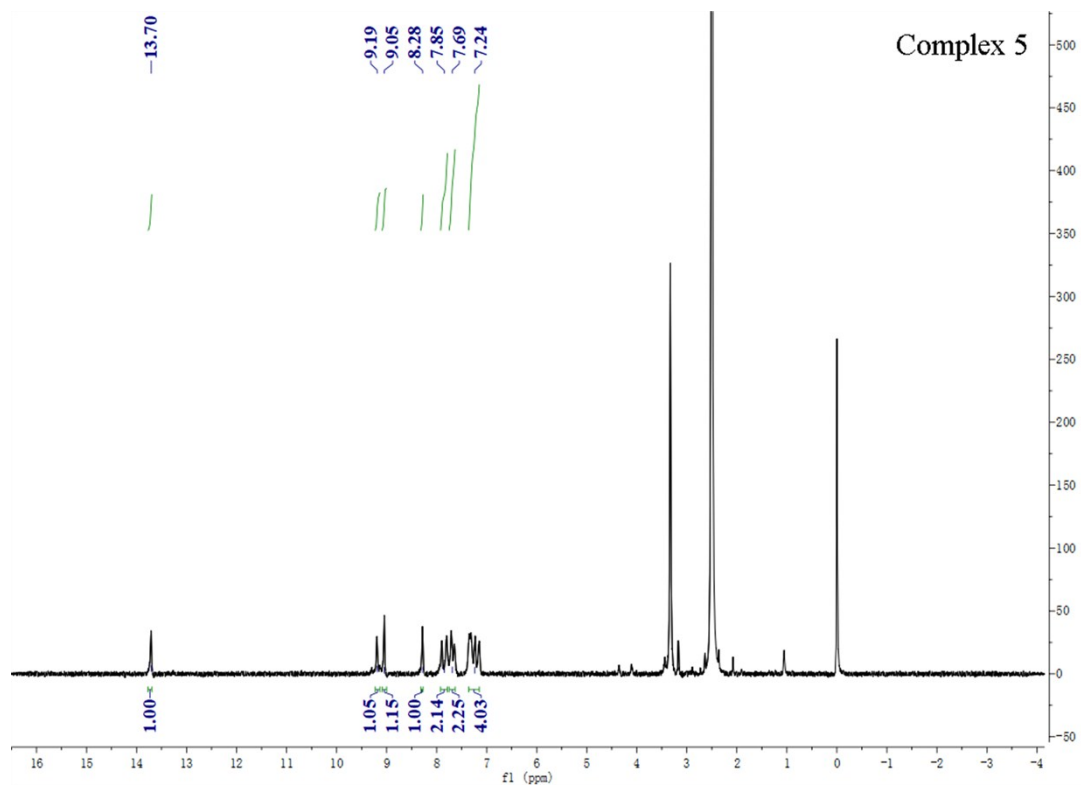
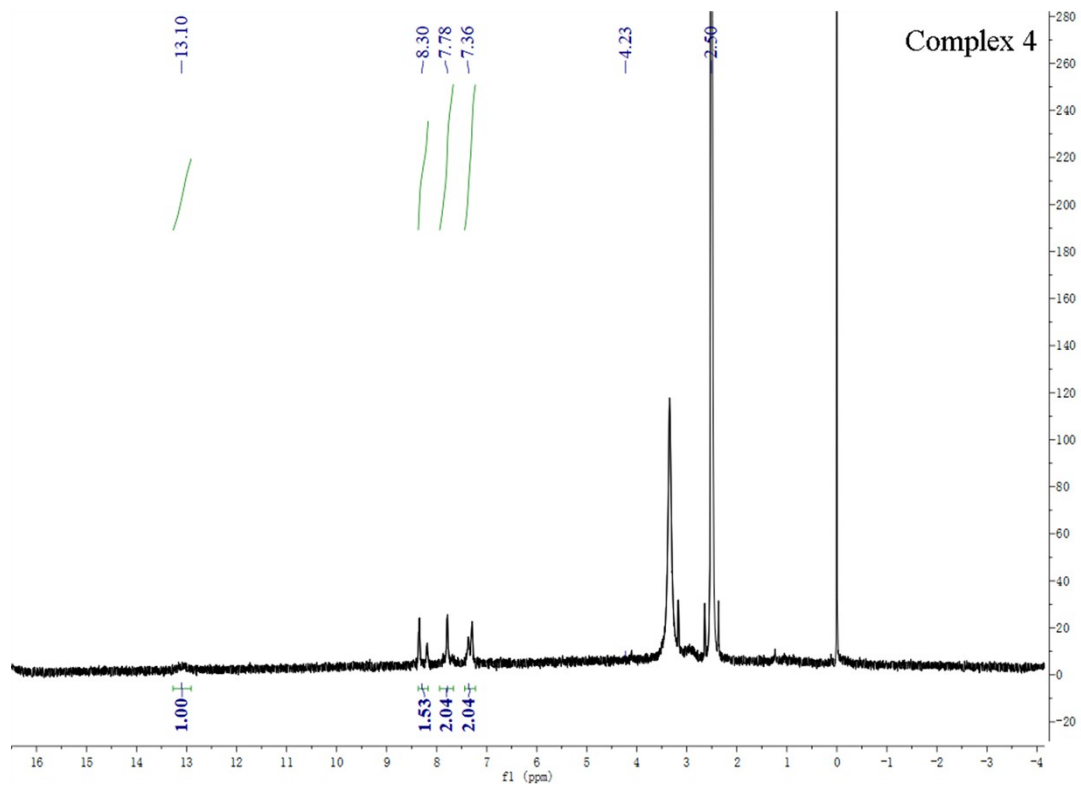
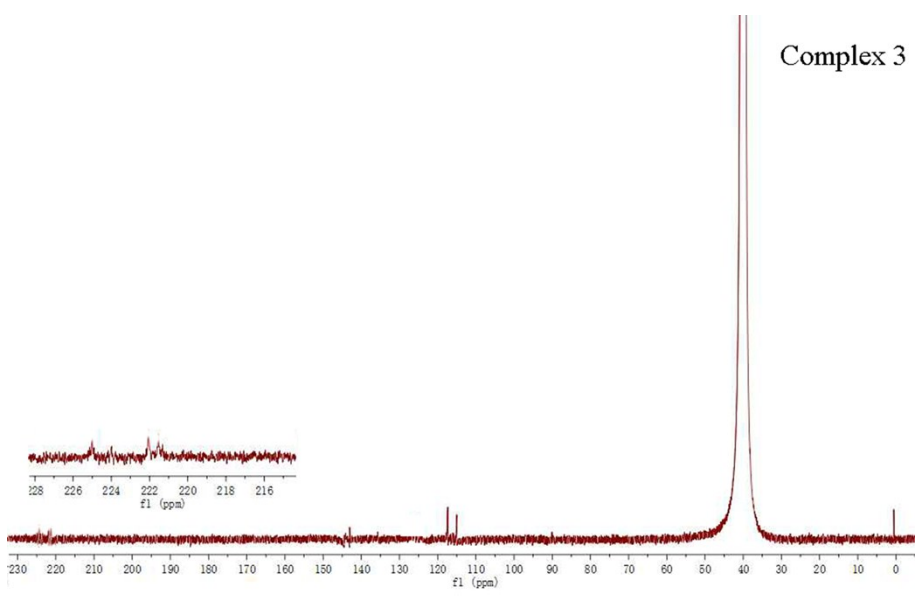
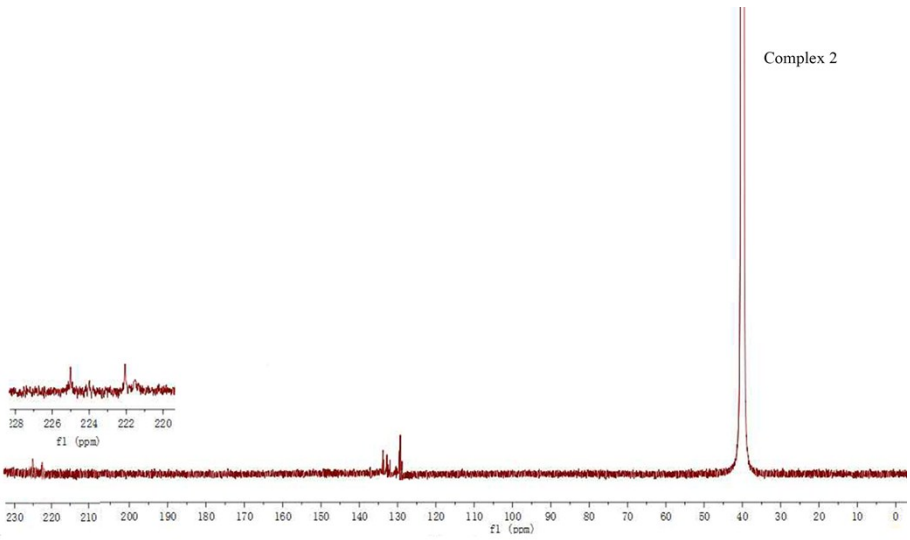
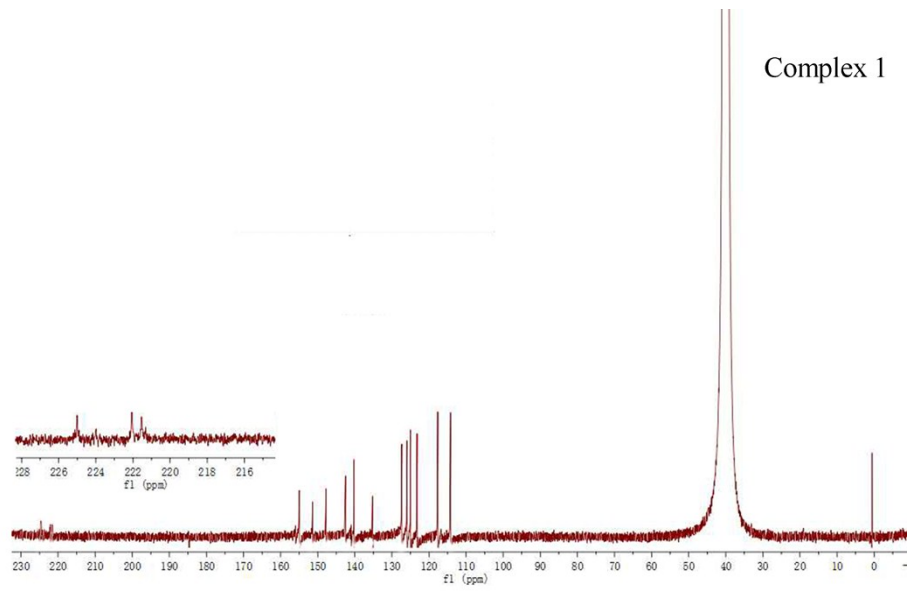


Fig. S3 $^1\text{H-NMR}$ spectra of complexes 1-5 in DMSO at 298 K.



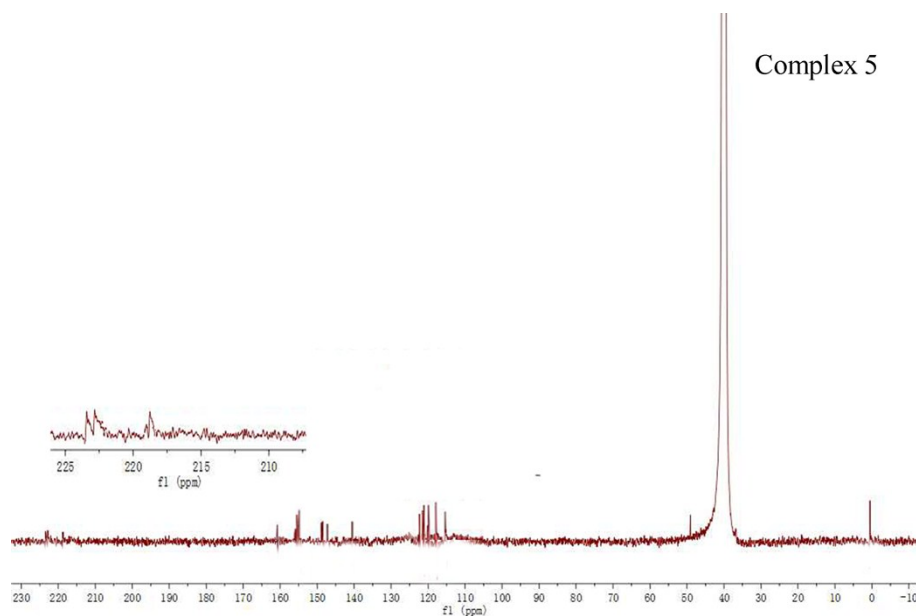
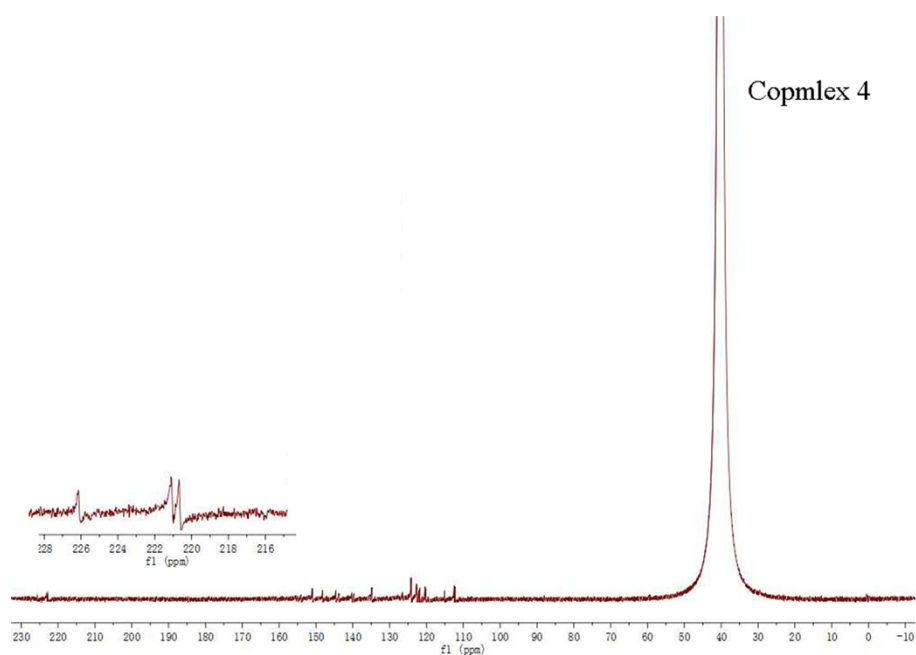


Fig. S4 ^{12}C -NMR spectra of complexes 1-5 in DMSO at 298 K.

Table S1. Crystal Data and Structure Refinement Parameters for complex 1-4

	1	2	3	4
Empirical formula	$\text{C}_{15}\text{H}_9\text{BrN}_3\text{O}_3\text{Mn}$	$\text{C}_{50}\text{H}_{39}\text{ClN}_5\text{O}_6\text{P}_2\text{Mn}$	$\text{C}_{17}\text{H}_{10}\text{BrN}_4\text{O}_3\text{Mn}$	$\text{C}_{23}\text{H}_{17}\text{BrN}_5\text{O}_4\text{Mn}$
Formula weight	414.10	930.17	453.13	562.26
Colour	Yellow	Pink	Yellow	Yellow
Crystal system	Triclinic	Triclinic	Monoclinic	Monoclinic
Space group	P-1	P-1	$\text{P2}_1/\text{c}$	$\text{P2}_1/\text{n}$
a (Å)	6.8422(3)	11.2347(7)	7.091(2)	7.2795(18)
b (Å)	10.6873(5)	12.2555(7)	18.276(6)	15.523(4)
c (Å)	11.6987(6)	16.4480(10)	13.255(4)	20.599(5)
α (deg)	91.775(3)	82.506(2)	90.00	90.00

β (deg)	105.866(3)	88.492(3)	96.754(6)	98.920(17)
γ (deg)	108.240(3)	77.515(2)	90.00	90.00
V (Å ³)	775.14(6)	2192.2(2)	1705.8(9)	2294.4(9)
Z	2	2	16	4
ρ_{calc} (g·cm ⁻³)	1.774	1.409	1.764	1.628
Independent reflections	3812	10902	3920	4042
Goodness of fit (F^2) ^a	1.041	1.036	0.930	0.980
R_1^b , wR_2^c ($I > 2\sigma(I)$)	0.0440, 0.1092	0.0353, 0.0914	0.0480, 0.0849	0.0949, 0.1432
R_1 , wR_2 (all data)	0.0575, 0.1173	0.0470, 0.0996	0.1025, 0.1019	0.2403, 0.1998
Largest diff. peak /hole/eÅ ⁻³	1.93/-0.35	0.44/-0.32	1.06/-1.22	0.51/-0.58

^aGOF = $[\sum(\omega(F_o^2 - F_c^2)^2)/(N_o - N_v)]^{1/2}$ (N_o =number of observations, N_v = number of variables). ^b $R_1 = \sum |F_o| - |F_c| / \sum |F_o|$. ^c $wR^2 = [(\sum \omega(|F_o|^2 - |F_c|^2)^2) / \sum \omega |F_o|^2]^{1/2}$.

Table S2. Selected bond lengths (Å) and bond angles (°) of complexes **1-4**.

1		2	
Mn(1)-Br(1)	2.5531(6)	Mn(1)-C(17)	1.7775(16)
Mn(1)-C(13)	1.808(4)	Mn(1)-C(47)	1.7895(16)
Mn(1)-C(14)	1.801(4)	Mn(1)-N(2)	2.0530(12)
Mn(1)-C(15)	1.790(4)	Mn(1)-N(1)	2.0769(13)
Mn(1)-N(1)	2.032(2)	Mn(1)-P(1)	2.3287(4)
Mn(1)-N(3)	2.093(3)	Mn(1)-P(2)	2.3279(4)
C(15)-Mn(1)-C(14)	87.89(17)	C(17)-Mn(1)-C(47)	95.05(7)
C(15)-Mn(1)-C(13)	90.82(18)	C(17)-Mn(1)-N(2)	170.40(6)
C(14)-Mn(1)-C(13)	88.83(18)	C(47)-Mn(1)-N(2)	94.54(6)
C(15)-Mn(1)-N(1)	172.32(15)	C(17)-Mn(1)-N(1)	92.18(6)
C(14)-Mn(1)-N(1)	98.21(13)	C(47)-Mn(1)-N(1)	172.65(6)
C(13)-Mn(1)-N(1)	93.96(13)	N(2)-Mn(1)-N(1)	78.24(5)
C(15)-Mn(1)-N(3)	95.45(15)	C(17)-Mn(1)-P(2)	88.92(5)
C(14)-Mn(1)-N(3)	176.56(13)	C(47)-Mn(1)-P(2)	89.54(5)
C(13)-Mn(1)-N(3)	91.94(14)	N(2)-Mn(1)-P(2)	90.83(4)
N(1)-Mn(1)-N(3)	78.39(10)	N(1)-Mn(1)-P(2)	91.95(4)
C(15)-Mn(1)-Br(1)	88.00(15)	C(17)-Mn(1)-P(1)	88.17(5)
C(14)-Mn(1)-Br(1)	89.90(14)	C(47)-Mn(1)-P(1)	88.22(5)
C(13)-Mn(1)-Br(1)	178.30(12)	N(2)-Mn(1)-P(1)	92.45(4)
N(1)-Mn(1)-Br(1)	87.35(8)	N(1)-Mn(1)-P(1)	90.67(4)
N(3)-Mn(1)-Br(1)	89.39(8)	P(2)-Mn(1)-P(1)	176.158(16)
3		4	
Mn(2)-Br(1)	2.5701(11)	Mn(2)-Br(1)	2.540(2)
Mn(2)-C(15)	1.803(5)	Mn(2)-C(12)	1.883(15)
Mn(2)-C(16)	1.813(5)	Mn(2)-C(22)	1.827(16)
Mn(2)-C(17)	1.7996(6)	Mn(2)-C(9)	1.806(12)
Mn(2)-N(4)	2.066(3)	Mn(2)-N(1)	2.051(10)

Mn(2)-N(1)	2.082(3)	Mn(2)-N(8)	2.150(10)
C(15)-Mn(2)-Br(1)	87.33(16)	C(22)-Mn(2)-C(9)	88.8(6)
C(16)-Mn(2)- Br(1)	90.12(16)	C(22)-Mn(2)-C(12)	86.2(6)
C(16)-Mn(2)-C(15)	88.9(2)	C(9)-Mn(2)-C(12)	90.2(5)
C(17)-Mn(2)- Br(1)	176.66(14)	C(22)-Mn(2)-N(1)	96.0(5)
C(17)-Mn(2)- C(15)	89.5(2)	C(9)-Mn(2)-N(1)	97.4(4)
C(17)-Mn(2)- C(16)	88.7(2)	C(12)-Mn(2)-N(1)	172.2(4)
N(4)-Mn(2)-Br1	88.87(10)	C(22)-Mn(2)-N(8)	174.1(4)
N(4)-Mn(2)-C(15)	96.18(17)	C(9)-Mn(2)-N(8)	94.6(5)
N(4)-Mn(2)-C(16)	174.77(17)	C(12)-Mn(2)-N(8)	98.5(5)
N(4)-Mn(2)-C(17)	92.62(18)	N(1)-Mn(2)-N(8)	78.9(4)
N(1)-Mn(2)-B1(1)	87.14(10)	C(22)-Mn(2)-Br(1)	86.1(4)
N(1)-Mn(2)-C(15)	172.15(17)	C(9)-Mn(2)-Br(1)	173.1(4)
N(1)-Mn(2)-C(16)	96.67(17)	C(12)-Mn(2)-Br(1)	84.7(3)
N(1)-Mn(2)-C(17)	96.09(17)	N(8)-Mn(2)-Br(1)	90.8(2)
N(1)-Mn(2)-N(4)	78.15(12)	N(1)-Mn(2)-Br(1)	87.9(2)

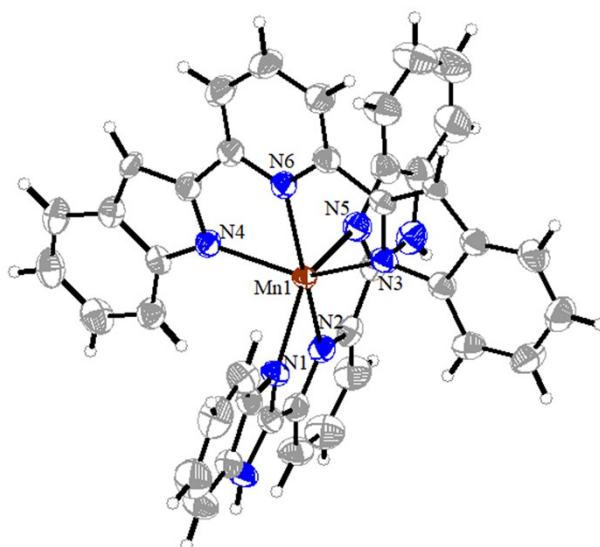


Fig. S5 Molecular structure of complex composed of Mn and L3.

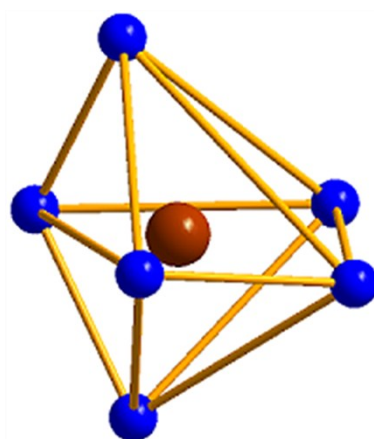


Fig. S6 Coordination Arrangement of the complex composed of Mn and L3.

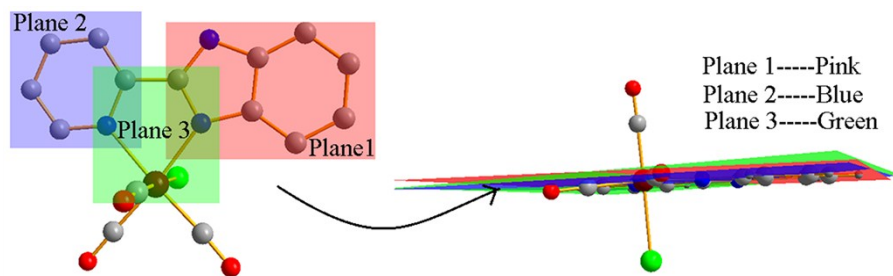


Fig. S7 The dihedral angle of plane 1, 2 and 3 in complex 1.

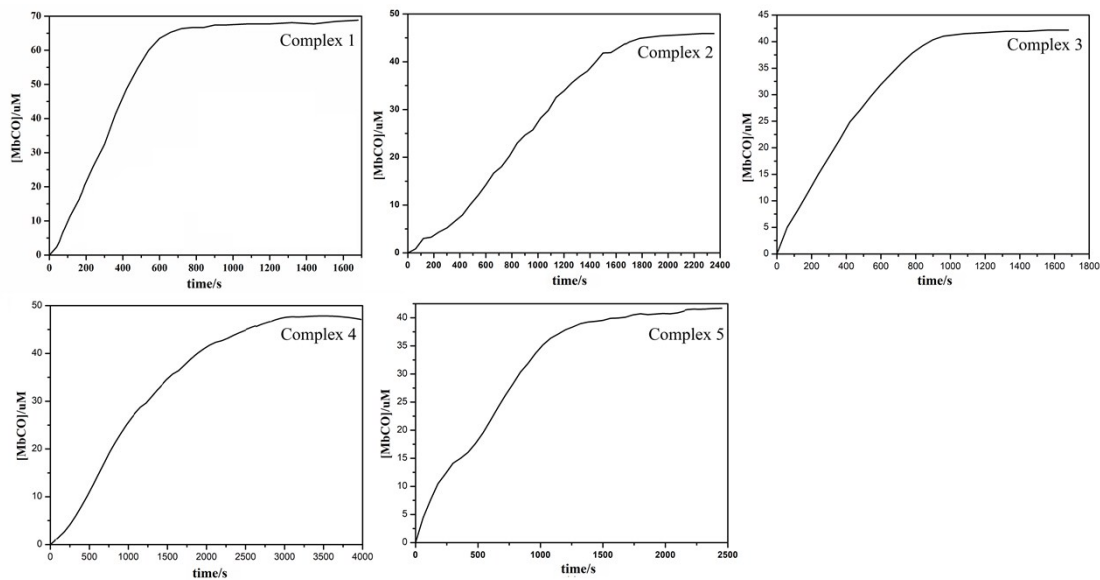


Fig. S8 Amount of MbCO in μM formed with increasing irradiation time at 365 nm for a solution of complexes 1-5 (60 μM in 0.1 PBS at pH 7.4) with sodium dithionite (10 mM) as determined from UV/vis spectroscopy.

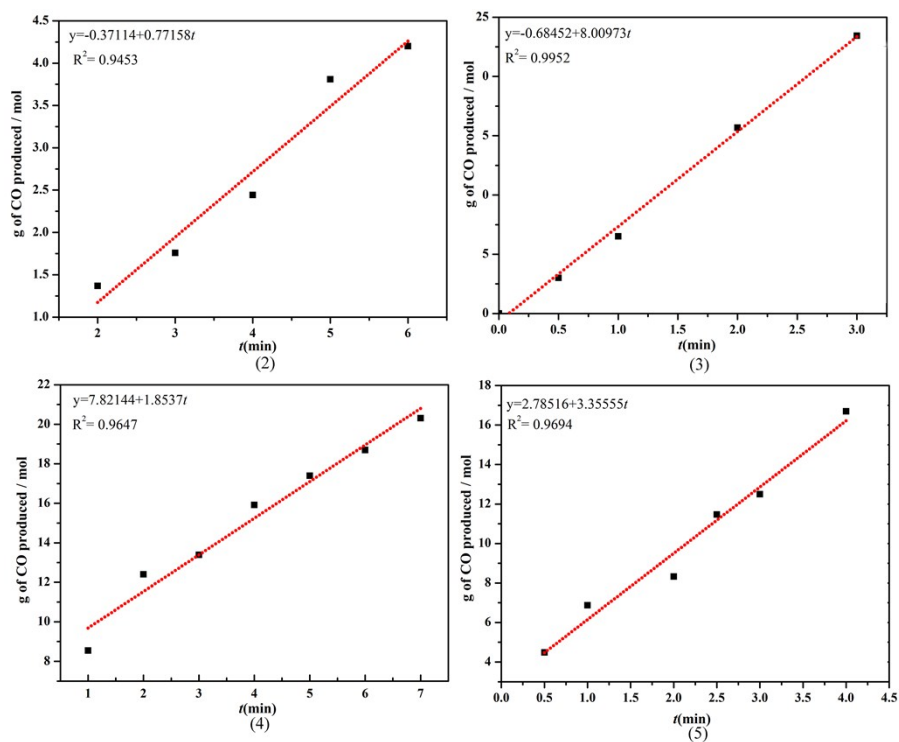


Fig. S9 The rates of CO produced (k_{CO}) for 2–5 by using a CO meter.

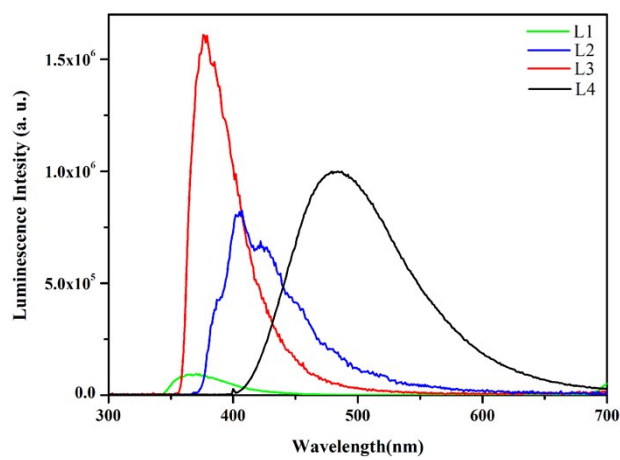
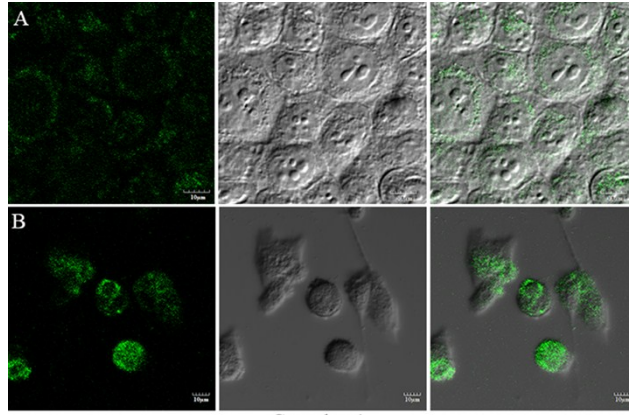
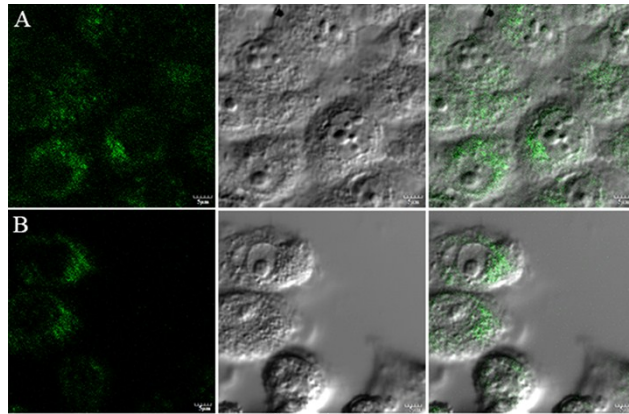


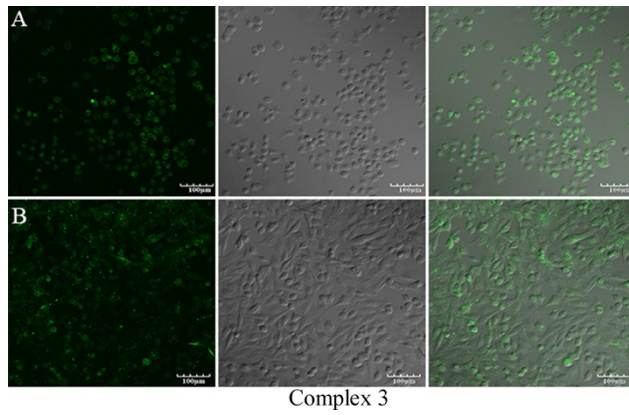
Fig. S10 The emission spectra of L1-L4 in DMSO at room temperature.



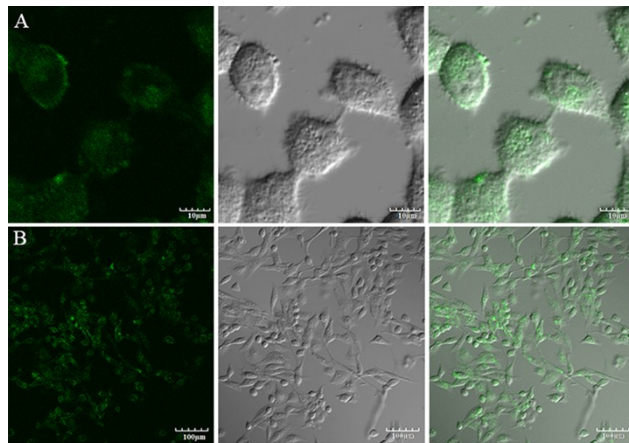
Complex 1



Complex 2



Complex 3



Complex 5

Fig. S11 Fluorescence imaging of live HL-7702 cells (A) and SK-Hep1 cells (B) after being incubated with complex 1-3, 5 for 2 h. The left panels show dark-field fluorescence images, the middle panels show the corresponding bright-field images and the right panels are overlays of the left and middle panels.